Bulletin of the Seismological Society of America, Vol. 105, No. 4, pp. –, August 2015, doi: 10.1785/0120150024

Ⓔ

WIGWAM Reverberation Revisited

by Brian D. Dushaw

Abstract Operation WIGWAM was a test of a 30 kt nuclear depth charge conducted in deep water 500 miles southwest of San Diego on 14 May 1955. Its primary purpose was to determine the effectiveness of that device as an antisubmarine weapon. The acoustic pulse from the test, initially an intense shockwave, radiated throughout the North and South Pacific Oceans. Acoustic reflections from topographic features were recorded for several hours after the explosion by SOund Fixing And Ranging (SOFAR) hydrophones at Point Sur, California, and Kaneohe, Hawaii. Sheehy and Halley (1957) identified peaks of the recorded coda with reflections from specific topographic features at great distances (e.g., the Hawaiian Islands, French Polynesia, or Fiji). With modern data for seafloor topography and ocean sound speed, these coda were computed with surprising accuracy using simple geodesic rays reflected from islands and seamounts. The intensity variations of the coda are mostly determined by simple ray geometry, together with modest attenuation. Coda peaks are often obtained from rays arriving simultaneously from multiple, but disparate, topographic features.

Online Material: Figures of computed and measured coda and associated geodesic paths.

Introduction

Operation WIGWAM was a test of a 30 kt nuclear depth charge conducted in deep water approximately 500 miles (800 km) west-southwest of San Diego on 14 May 1955. Its primary purpose was to determine the effectiveness of such a device as an antisubmarine weapon. The test also involved extensive scientific and military programs, including radiological and oceanographic studies (Department of Defense, 1955; see Data and Resources; Focke, 1958; Weary *et al.*, 1981). WIGWAM was the first detonation of a nuclear device in deep water (16,000 ft [4877 m]), and it remains the only such test in water deeper than 1000 m.

The WIGWAM detonation generated an intense acoustic shock wave within the ocean, of course, and the resulting acoustic pulse was of such intensity that both the North and South Pacific Oceans were strongly acoustically illuminated. The reflections of this sound energy from distant topographic features such as islands, ridges, or seamounts were of sufficient intensity that they were recorded as hours-long coda at SOund Fixing And Ranging (SOFAR) stations at Kaneohe, Hawaii, and Point Sur, California. The maximum recorded travel times correspond to total propagation distances of approximately 20,000 km. Sheehy and Halley (1957) analyzed these data to estimate the frequency dependence of sound attenuation at low frequencies. The recorded coda consisted of a sequence of well-defined peaks, and Sheehy and Halley identified these peaks as corresponding to reflections from specific topographic features at great ranges from the WIGWAM location (Fig. 1). The WIGWAM reverberation is an extraordinary example of the general problem of reverberation of low-frequency acoustic signals by topographic features, reviewed by Baggeroer and Dyer (1986). Upton *et al.* (2006) describe a model for computing arrival coda from reflected hydroacoustic signals propagating over long distances in the ocean.

This article examines the outgoing and reflected acoustic paths from the WIGWAM test, with the aims of computing the recorded coda and determining the accuracy of the peak identifications of Sheehy and Halley (1957). The simplest of acoustic models, geodesic paths along the sound-channel axis, was used to reconstruct the coda to considerable accuracy. To some extent, one of the main points of this article is to show that this simple model is both entirely justified and (un)surprisingly accurate, based on the results derived from a program on ocean acoustic thermometry in the North Pacific over the past 15 years (Worcester and Spindel, 2005; Dushaw *et al.*, 2009). The Sheehy and Halley (1957) interpretation was found to be essentially correct, with occasional corrections to the origins of the identified peaks. The Acoustic Source and Receivers section describes the properties of the WIGWAM detonation as an acoustic source and the parameters of the acoustic receivers. The Simplifying Assumptions section describes the motivations and justifications for a number of simplifying assumptions, leading to

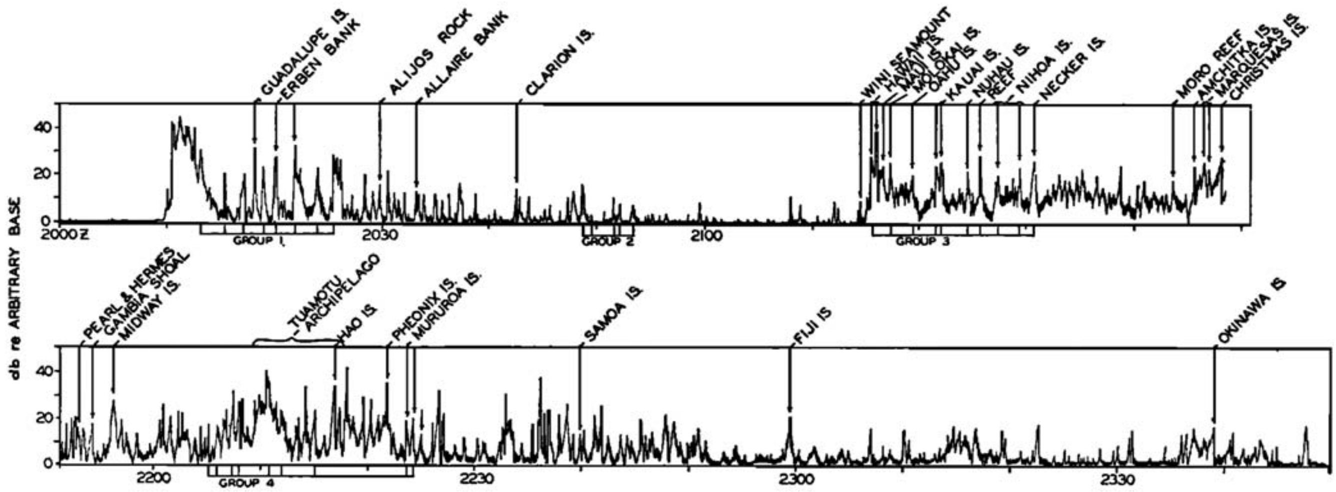

Figure 1. Coda of WIGWAM acoustic reverberations recorded by the hydrophone array off Point Sur, California. Sheehy and Halley (1957) identified recorded peaks as reflections from particular islands or seamounts at one-way ranges of up to approximately 10,000 km. A gap in the record of several minutes duration occurs at approximately the 21:50 time, between the panels. (Reprinted with permission from Sheehy and Halley, 1957, copyright 1957, Acoustical Society of America.)

the simple geodesic path model. The Ocean Environment section describes the ocean environment, that is, the topographic database and sound speed derived from ocean climatology. The Computed Coda section describes the outward bound and reflected acoustic paths and shows how the coda stemming from these reflected paths was computed for comparison to the observations. Throughout this article, units of essential quantities are reported as they were recorded at the time, but converted to the meters-kilograms-second (MKS) system of units in parentheses. In the ocean acoustics community low frequency usually refers to frequencies 0(100 Hz), in contrast to the usage of the seismology community.

Acoustic Source and Receivers

Because WIGWAM was a carefully planned experiment, two essential parameters required of an acoustic source are well known, namely the timing and position of the detonation. The detonation occurred at 12:59:59.884 Pacific Daylight Time, or very nearly 20:00:00 Coordinated Universal Time (Department of Defense, 1955; see Data and Resources). The position of the shot was 28°44′ N 126°16′ W with an uncertainty of 1 min. The position uncertainty corresponds to a range uncertainty of approximately 1 nm, or acoustic travel-time uncertainty of approximately 1 s. The position would have been determined by celestial navigation, which under the best of conditions has an uncertainty of 1 min. The shot was detonated at a depth of 2000 ft (610 m). The acoustic source level was, to say the least, intense. A ship off the coast of San Francisco at the time of detonation reported being "shaken up" by a great disturbance (Department of Defense, 1955). Convinced that San Francisco had suffered a major earthquake, the ship radioed to offer assistance.

The acoustic energy was generated by possibly three mechanisms. The dominant source of energy was likely the initial shock wave, which is readily apparent on the ocean surface in films of the test. The explosion then created a bubble that was calculated to have a maximum radius of 376 ft (115 m). This bubble pulsated with period of ∼2.88 s, and the bubble pulsed three times before reaching the surface (Focke, 1958). Lastly, the blast displaced an enormous quantity of water into the atmosphere. Occurring in distinct waves, the water thrown into the atmosphere reached a height of approximately 900 ft (274 m). Inasmuch as the only acoustic data available for this study were given in the figure of the coda reported by Sheehy and Halley (1957) (Fig. 1), all of these sources of acoustic energy are essentially simultaneous given the best temporal resolution afforded by the figure. The best working resolution for acoustic travel time in this study, determined by the resolution of the scanned figure, is approximately 30 s. However, if the original data for the coda could be located, a travel-time precision of 10–100 ms could likely be obtained. The largest source of uncertainty is likely the shot position.

The reverberations recorded by the SOFAR hydrophones had frequencies that ranged from 10 to 200 Hz, peaking at around 40 Hz (Sheehy and Halley, 1957). Although the initial shock wave corresponds to a white frequency spectrum, frequencies of sound $>$100–200 Hz are rapidly attenuated with range (Dushaw and Menemenlis, 2014).

Both the Kaneohe and Point Sur receivers were located at approximately 400 fathoms (732 m) depth, which is near the sound channel axis at those locations. Two additional hydrophones at Point Sur at 60 fathoms (110 m) depth were also used by Sheehy and Halley (1957). The Kaneohe hydrophone location is located at approximately 21.820° N, 157.950° W (McDonald and Fox, 1999). The Point Sur hydrophone facility operated until the mid-2000s, and the location of the receiver was 36.302° N, 122.394° W (Dushaw *et al.*, 2009). This position is not likely to be identical to the location of the hydrophone in 1955, but any likely difference

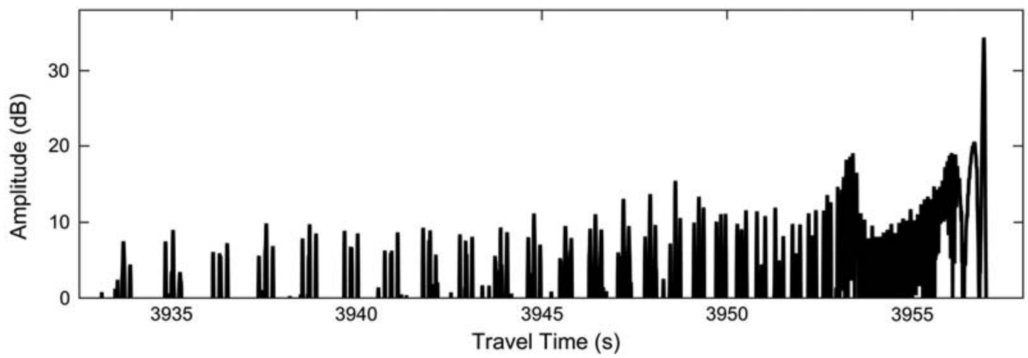

Figure 2. Nominal acoustic arrival pattern, or impulse response, for 75 Hz acoustic propagation from the WIGWAM site to a point near the Emperor Seamount Chain, range of 5844 km, computed using the 2009 World Ocean Atlas and the parabolic equation technique. This pattern occurs at 500 m depth, corresponding to the sound channel axis at the seamount chain. The final peak, which is the first acoustic mode, is approximately 25 dB more intense than earlier, deep-turning, ray arrivals.

is negligible for our purposes. A 10 km error in position corresponds to only 7 s travel-time error.

Simplifying Assumptions

At first glance, the task of computing the recorded coda appears to be formidable, but a variety of simplifying assumptions can be made that render the essential nature of the problem almost trivial. Formally, the rigorous computational task would involve computing the propagation of broadband acoustic signals by employing a 3D acoustic model that could account for the horizontal refraction caused by ocean variability and shoaling topographic features (Jensen *et al.*, 1994). When these signals encountered a topographic termination, a model for the reflection of those signals would have to be employed, accounting for complications such as scattering or attenuation from local geophysical conditions. The propagation of the reflected signals would then have to be computed to finally obtain time series of acoustic intensity at the receiver locations. One might then be skeptical that the ocean conditions were adequately estimated. Are the oceanographic features that cause refraction adequately represented? What is the magnitude of the effects of ocean variability on acoustic travel times over basin scales? Are ocean conditions estimated today sufficiently similar to those encountered in 1955?

The results from a decade-long program employing ocean acoustic thermometry in the Pacific Ocean show that these complications and concerns are mostly moot. The sound speed environment of the deep ocean is both remarkably stable and well defined (Worcester *et al.*, 1999; Dushaw *et al.*, 2009, 2013; Dushaw and Menemenlis, 2014). Travel times of acoustic signals over 5 Mm ranges in the Pacific Ocean vary by less than ± 0.5 s over decadal time scales (Dushaw *et al.*, 2009, 2013). Horizontal refraction of those signals, from either oceanographic or topographic features, are mostly inconsequential (Munk and Zachariasen, 1991; Dushaw, 2014; Dushaw and Menemenlis, 2014), certainly inconsequential for the simple calculation employed here. Finally, the acoustic signals are dominated by propagation confined near the sound channel axis. As Figure 2 illustrates, acoustic energy that turns in the deep ocean becomes dispersed in time, eventually rendering the acoustic energy confined near the sound channel axis, the low acoustic modes, relatively more intense than any other signals. Figure 2 employs the example of acoustic propagation over a 5.8 Mm long acoustic path between the WIGWAM location and the Emperor Seamount chain in the central North Pacific Ocean. In this example, the on-axis acoustic energy has a signal level approximately 25 dB greater than most other acoustic features. The coda reported by Sheehey and Halley (Fig. 1) can be considered an accumulation of such low-mode, high-amplitude arrivals.

These considerations suggest the simplest possible acoustic model: simple geodesic paths along the sound channel axis (see also Munk *et al.*, 1988). The conjecture is that the variations in acoustic amplitude shown in the recorded coda ultimately resulted from simple ray geometry, with greater amplitude corresponding to more arriving acoustic paths. Although acoustic mode phase speeds have been employed for calculations like this (Heaney *et al.*, 1991; Dushaw and Menemenlis, 2014), the complications of acoustic modes are avoided here to keep the analysis focused on the geometrical aspects of the problem. Such complications include the nonadiabatic mode propagation at 0(40 Hz) frequencies, the frequency dependence of the mode shapes, and the requirement for a model to account for the reflection of modes from topographic features. Travel times computed for paths on the sound channel axis are reasonably accurate, certainly within the 30 s precision stated above. In the example of Figure 2, the travel time along the sound channel axis is 3957.4 s, which is within 1 s of the travel times of the final arrival. The acoustic propagation was therefore modeled as a dense set of omnidirectional geodesic paths emanating from the WIGWAM location, traversing the ocean along the sound channel axis, and terminating where the ocean seafloor intersects the sound channel axis (Fig. 3). Geodesic paths then reflect back from those termination points to the locations of the Kaneohe or Point Sur receivers, except those return paths obstructed by topographic features. The reflection of these

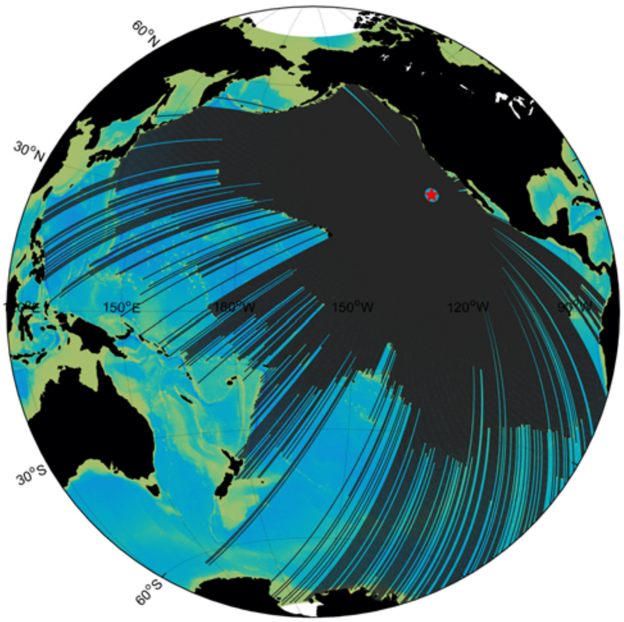

Figure 3. The acoustic energy from the WIGWAM test illuminated most of the North and South Pacific basins. Acoustic rays here terminate where undersea ridges or islands intersect the sound channel axis. Significant energy would have reached the Antarctic continent, and a small set of rays south of New Zealand indicates that at least some acoustic energy escaped into the southern Indian Ocean. Azimuthal equal area projection. The color version of this figure is available only in the electronic edition.

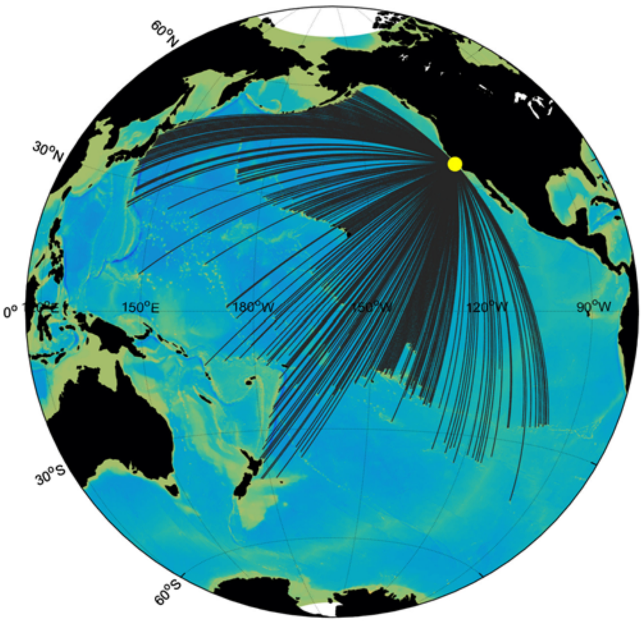

Figure 4. Acoustic energy was reflected from topographic features back to the receiver at Point Sur, California, as indicated by the ray paths. Only ray paths with total range <10.6 Mm are shown because the reported coda record length only extends to 3.8 hrs. The return rays indicated here have avoided topographic obstruction to arrive at the Point Sur receiver. It is likely that significant acoustic energy was reflected from Antarctica back to the Point Sur receiver. The color version of this figure is available only in the electronic edition.

acoustic signals is assumed to be specular, with local roughness sufficient to impart a significant signal back in the direction of the receiver. We appeal to the success of the model in justifying these latter assumptions regarding the topographic interaction.

Ocean Environment

A representation for the ocean sound speed environment can be obtained using the National Oceanic and Atmospheric Administration's World Ocean Atlas (WOA) (Antonov *et al.*, 2009; Locarnini *et al.*, 2009). This 1° horizontal resolution atlas comprises estimates for the annual mean temperature and salinity fields of the world's oceans. The atlas employs 33 standard depths, extending to 5500 m. Pressure was first computed from the depth, temperature, and salinity variables, and then sound speed was computed using the Del Grosso (1974) equation. The annual mean WOA sound speeds accurately represent the zero-order environment for acoustic propagation (Worcester *et al.*, 1999; Dushaw *et al.*, 2013), perhaps better than any other model.

The Smith–Sandwell global seafloor topography (v.14.1, Smith and Sandwell, 1997) was used as the model for the seafloor. This 1 min resolution topographic estimate from the University of California, San Diego, is determined by satellite altimetry and gravity data together with *in situ* ship soundings and multibeam data.

Computed Coda

As introduced above, geodesic paths, employing the WGS'84 reference coordinate system, were computed for a large number of azimuthal directions emanating from the point of the WIGWAM detonation. Azimuthal angle increments of 0.025° were employed, giving 14,400 geodesic paths (Fig. 3). Such a dense set of geodesics was required to ensure the paths intersected with most, if not all, topographic features as small as isolated seamounts. These paths continued to whatever range was required for them to intersect the seafloor topography at the depth of the sound channel minimum. The sound speed along each path at the depth of the sound channel minimum was then computed and used to compute acoustic travel time along the path. From each point of intersection with the topography, return geodesic paths and travel times to the receiver locations were then computed. Return paths that were obstructed by other topographic features before arriving at a receiver location or that were longer than 10.6 Mm range were omitted (Fig. 4). Paths with ranges longer than 10.6 Mm have total travel times longer than the available record length, 3.8 hr. The set of rays arriving at the receiver location has a corresponding set of travel times that depend on the range and the sound speed averaged over the path along the sound channel axis. This set of travel times was histogrammed, with the number of rays in each travel-time bin assumed to correspond to an estimate for the acous-

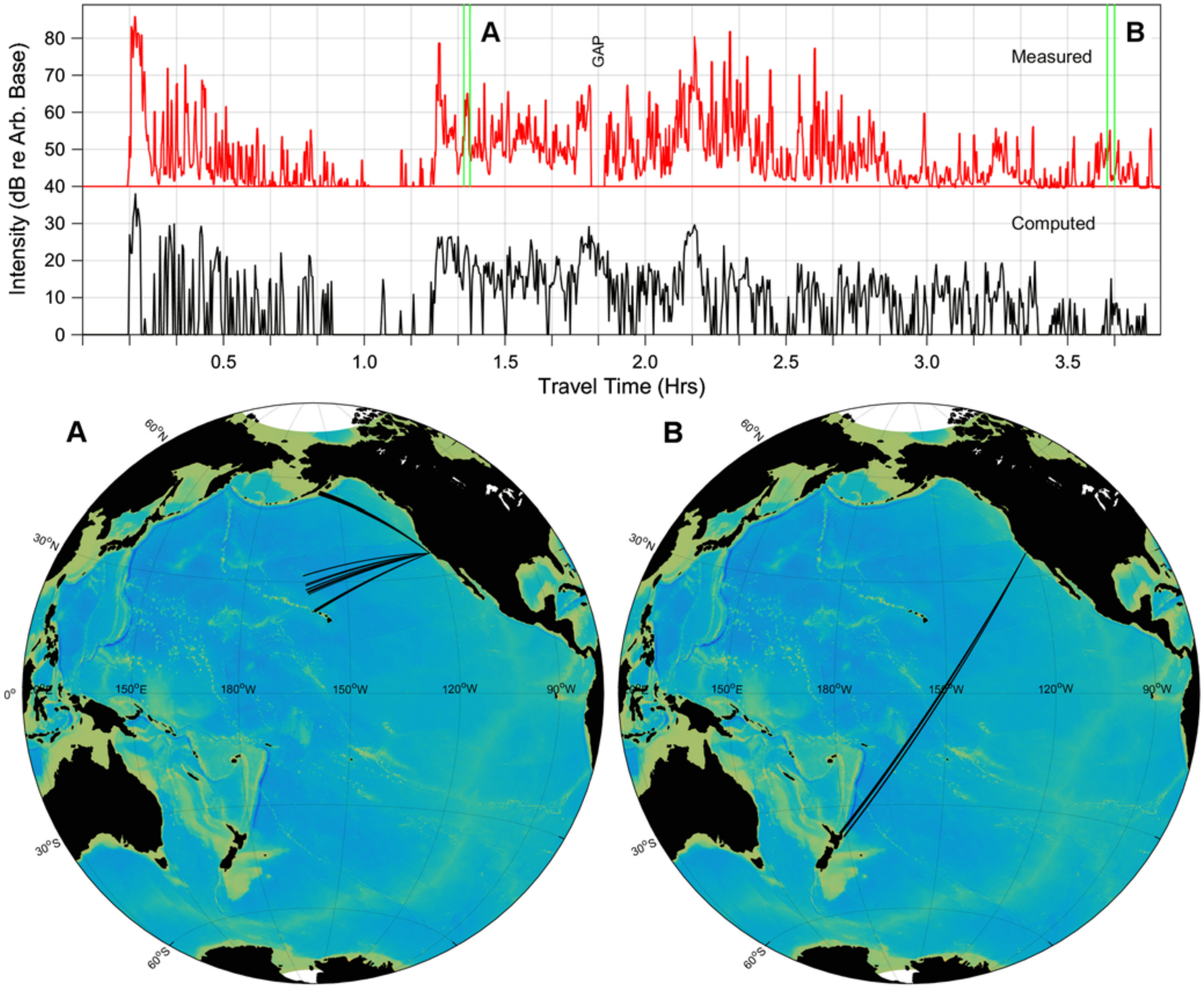

Figure 5. The coda for the location of the receiver off Point Sur, California, computed from simple geodesic paths corresponds remarkably well with the measured coda as indicated in the top panel. The measured coda was digitized from the figure from Sheehy and Halley (1957) (see Fig. 1), which had a gap in the record at approximately the 1.8 hr time, as indicated. The acoustic peak denoted A in the top panel was identified by Sheehy and Halley (1957) as originating from a reflection from Kauai, Hawaii, but this feature also included contributions from the Aleutians and seamounts north of Hawaii (lower left). The acoustic peak denoted B was identified by Sheehy and Halley (1957) as resulting from a reflection from Okinawa Island, Japan, but this feature resulted from reflection from the north coast of New Zealand (lower right). Ⓔ A complete set of acoustic paths corresponding to recorded features can be seen in the electronic supplement to this article. The color version of this figure is available only in the electronic edition.

tic amplitude (Figs. 5 and 6). The intensity on a decibel scale was computed as $A(t) = 15 \log N(t)$, in which $N(t)$ was the number of rays occurring in the travel-time bin at time t, and the factor 15 was selected by trial and error for optimal overall alignment with the observations. The estimated relative acoustic amplitudes are therefore determined entirely by ray path geometry or density.

Two refinements to this simple scheme were required. First, although the correspondence between the computed and measured coda were remarkably good (Figs. 5 and 6), the computed amplitudes for the later arrivals were significantly larger than measured. This discrepancy was readily accounted for by applying a simple attenuation factor of 0.0001 dB per kilometer of range, a value roughly appropriate for the low frequencies of these acoustic signals (e.g., Sheehy and Halley, 1957; Jensen *et al.*, 1994). Second, almost no reflections were obtained at relatively short travel times at approximately the half-hour mark in the Point Sur coda. As noted by Sheehy and Halley (1957), arrivals in this time interval were caused by reflections from unknown deep seamounts in the eastern Pacific basin, at a relatively short range from the WIGWAM site. To account for deep seamounts, a second set of geodesic paths was computed to topographic points at 1500 m depth, and these paths were combined with the sound channel axis paths. Although 1500 m is below the depths for low-order modes in the eastern

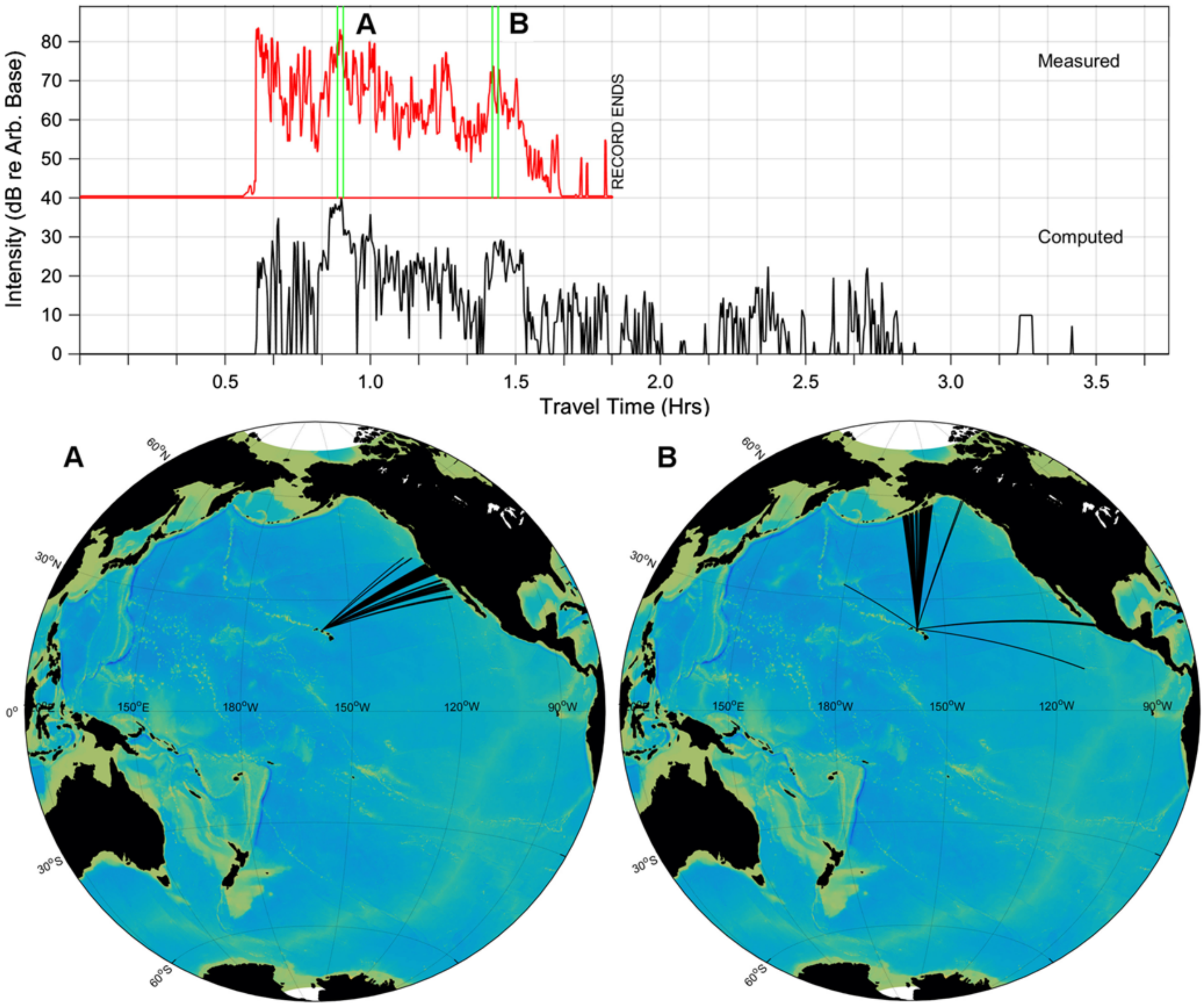

Figure 6. The coda for the location of the receiver off Kaneohe, Hawaii, computed from simple geodesic paths also corresponds remarkably well with the measured coda as indicated in the top panel. The measured coda was digitized from the figure from Sheehy and Halley (1957), for which the record terminated at approximately the 1.8 hr time, as indicated. The peak in the record denoted by A was identified by Sheehy and Halley (1957) as due to reflections from Point Conception, California, in rough agreement with the computed ray paths. The acoustic feature denoted B was identified as due to reflections from Socorro Island, Mexico, and Queen Charlotte Island, British Columbia, but this feature is mostly due to reflections from the Aleutian Islands. Ⓔ A complete set of acoustic paths corresponding to recorded features can be seen in the electronic supplement to this article. The color version of this figure is available only in the electronic edition.

North Pacific, the propagation ranges for these paths were fairly short. Short-range acoustic propagation allows for relatively minimal dispersal of an acoustic signal over time; hence in the arrival coda for short-range paths, deep-turning acoustic energy is of comparable intensity with on-axis acoustic energy. The two sets of geodesic paths, together with the modest range-dependent attenuation, gave computed coda in remarkably good agreement with the observations. Ⓔ A set of figures showing a detailed comparison between measured and computed coda for the Point Sur observations can be seen in the electronic supplement to this article.

From the ray arrivals that comprise specific peaks of the computed coda, the associated ray paths can be readily obtained. The lower panels of Figures 5 and 6 give examples for the Point Sur and Kaneohe receptions. The original identifications of Sheehy and Halley (1957) formed a reasonable first guess for the identification of peaks with specific topographic features, but the calculations here show the origins of the peaks are often not so simple. Ⓔ A complete set of acoustic paths corresponding to features of the entire Point Sur or Kaneohe coda can be seen in the electronic supplement to this article. The peaks identified by Sheehy and Halley (1957) in the Point Sur coda as originating from reflections from the Hawaiian Islands include significant contributions from reflections from the Aleutians as well. The two groups of paths have identical travel times. The peak identified as a reflection from Fiji Island appears to be correct, but the peak identified as from Okinawa Island was instead caused by reflections from the north coast of New Zealand. Significant reflections from undersea ridge systems are readily apparent. The Smith–Sandwell topographic data include many undersea features that were unknown in 1957.

Conclusions

On the one hand, the ability of the geodesic ray model to reproduce the measured coda is surprising, given the number of approximations and simplifications. On the other hand, these simplifications are well justified by the known stability and well-defined nature of the ocean's sound speed. The basic properties of acoustic propagation over basin-scale ranges are now fairly well known, experimentally and computationally. One motivation for this study was to test the conjecture that the simple geodesic path model would constitute a good zero-order approach to computing the coda. The least-justified assumption was that the reflection from islands, seamounts, or continental shelves was specular, omnidirectional, and independent of local geophysical conditions.

Another motivation for this study was to determine the accuracy of the peak identifications by Sheehy and Halley (1957) with specific topographic features. These identifications proved to be mostly correct, with some important differences. The most significant difference was that the features of the recorded coda were often a result of reflections from several disparate topographic features, rather than single isolated islands. For example, reflections from the Hawaiian Islands arriving at the Point Sur receiver were coincident with reflections from the Aleutian Islands. The notable reflection from the north coast of New Zealand, at approximately 20 Mm round-trip range, was not anticipated by Sheehy and Halley (1957). It seems evident that if a longer record length was available for the Point Sur coda, reflections from the Antarctic continent would have been apparent. Although Sheehy and Halley (1957) may not have been completely correct in their identifications, any errors were inconsequential to their determination of sound attenuation, because the acoustic energy corresponds to the sum of pulses traveling approximately the same range. Whether along a single path or several paths, the acoustic pulses experience the same attenuation because it depends only on range to first order.

Given the success of the simple model in computing coda similar to the observations, it seems evident that a more rigorous acoustical calculation may be able to compute coda that agree with the observations in every detail. Such a calculation may require 3D methods applied to broadband low-frequency acoustic signals, but such computations still require formidable computing resources. Given how well determined the ocean acoustic propagation problem is, this calculation may well offer an intriguing approach to understanding the interaction of low-frequency acoustic signals with topographic features. Such interactions are perhaps the least well-understood process here (see Baggeroer and Dyer, 1986), and they might require detailed knowledge of geophysical properties at the locations of interaction. In addition, a detailed calculation may require consideration of multiple reflections of the acoustic energy and the generation of T-phase signals from the seismic effects of the atomic test. The 3.8 hr coda offers an extraordinary amount of information about long-range, low-frequency acoustic propagation and its interaction with the seafloor. The greatest weakness of such a study may be the absence of the original recordings of the coda. A preliminary inquiry by the Marine Physical Laboratory in San Diego, the present-day institution of Sheehy and Halley (1957) and the organization that coordinated the scientific program for the WIGWAM test in 1955, was not successful in locating any of the original data.

Data and Resources

The global estimates for annual mean temperature and salinity fields for the oceans were obtained from the website for the 2009 World Ocean Atlas (Antonov *et al.*, 2009; Locarnini *et al.*, 2009; https://www.nodc.noaa.gov/OC5/WOA09/pr_woa09.html; last accessed May 2015).

The data for the Smith–Sandwell topography v.14.1 with 1 min resolution (Smith and Sandwell, 1997) were obtained from the website for these data at the Scripps Institution of Oceanography, University of California, San Diego (http://topex.ucsd.edu/marine_topo/; last accessed May 2015).

The mapping graphics software employed was M_Map, a mapping package for MATLAB by R. Pawlowicz at the University of British Columbia, Vancouver, Canada. This software package included the routines used to compute geodesic paths, based on the algorithm of Vincenty (1975) (http://www2.ocgy.ubc.ca/~rich/map.html; last accessed May 2015).

The Department of Defense (1955) "Nuclear Test Film—Operation WIGWAM," produced by the U.S. Air Force Lookout Mountain Laboratory, narrated by A. B. Focke, is available at https://archive.org/details/gov.doe.0800018 (last accessed May 2015).

Acknowledgment

The author was supported by Office of Naval Research Grants N00014-09-1-0446 and N00014-12-1-0183.

References

Antonov, J. I., D. Seidov, T. P. Boyer, R. A. Locarnini, A. V. Mishonov, H. E. Garcia, O. K. Baranova, M. M. Zweng, and D. R. Johnson (2009). *World Ocean Atlas 2009, Salinity*, Vol. 2, NOAA Atlas NESDIS 68, U.S. Government Printing Office, Washington, D.C., 184 pp.

Baggeroer, A. B., and I. Dyer (1986). Long range, low frequency acoustic backscattering: A survey, in *Ocean Seismo-Acoustics: Low-frequency Underwater Acoustics*, T. Akal and J. M. Berkson (Editors), Springer, New York, New York, 313–326, doi: 10.1007/978-1-4613-2201-6.

Del Grosso, V. A. (1974). New equation for the speed of sound in natural waters (with comparisons to other equations), *J. Acoust. Soc. Am.* **56,** 1084–1091.

Dushaw, B. D. (2014). Assessing the horizontal refraction of ocean acoustic tomography signals using high-resolution ocean state estimates, *J. Acoust. Soc. Am.* **136,** 1–8, doi: 10.1121/1.4881928.

Dushaw, B. D., and D. Menemenlis (2014). Antipodal acoustic thermometry: 1960, 2004, *Deep-Sea Res. I* **86,** 1–20, doi: 10.1016/j.dsr.2013.12.008.

Dushaw, B. D., P. F. Worcester, M. A. Dzieciuch, and D. Menemenlis (2013). On the time-mean state of ocean models and the properties of long-range acoustic propagation, *J. Geophys. Res. Oceans* **118,** doi: 10.1002/jgrc.20325.

Dushaw, B. D., P. F. Worcester, W. H. Munk, R. C. Spindel, J. A. Mercer, B. M. Howe, K. Metzger Jr., T. G. Birdsall, R. K. Andrew, M. A. Dzieciuch, *et al.* (2009). A decade of acoustic thermometry in the North Pacific Ocean, *J. Geophys. Res.* **114,** C07021, doi: 10.1029/2008JC005124.

Focke, A. B. (1958). Operation WIGWAM, Scientific Director's Summary Report, *Technical Report WT-1003 EX-1980*, Defense Nuclear Agency, Extracted Version, (AD No. 995030), 10 October 1958, 184 pp.

Heaney, K. D., W. A. Kuperman, and B. E. McDonald (1991). Perth-Bermuda sound propagation (1960): Adiabatic mode interpretation, *J. Acoust. Soc. Am.* **90,** 2586–2594.

Jensen, F. B., W. A. Kuperman, M. B. Porter, and H. Schmidt (1994). *Computational Ocean Acoustics*, American Institute of Physics, Woodbury, New York.

Locarnini, R. A., A. V. Mishonov, J. I. Antonov, T. P. Boyer, H. E. Garcia, O. K. Baranova, M. M. Zweng, and D. R. Johnson (2009). *World Ocean Atlas 2009, Temperature*, Vol. 1, NOAA Atlas NESDIS 68, U.S. Government Printing Office, Washington, D.C., 184 pp.

McDonald, M. A., and C. G. Fox (1999). Passive acoustic methods applied to fin whale population density estimation, *J. Acoust. Soc. Am.* **105,** 2643–2651.

Munk, W. H., and F. Zachariasen (1991). Refraction of sound by islands and seamounts, *J. Atmos. Ocean. Tech.* **8,** 554–574.

Munk, W. H., W. C. O'Reilly, and J. L. Reid (1988). Australia–Bermuda sound transmission experiment (1960) revisited, *J. Phys. Oceanogr.* **18,** 1876–1898.

Sheehy, M. J., and R. Halley (1957). Measurement of the attenuation of low-frequency underwater sound, *J. Acoust. Soc. Am.* **29,** 464–469.

Smith, W. H. F., and D. T. Sandwell (1997). Global seafloor topography from satellite altimetry and ship depth soundings, *Science* **277,** 1957–1962.

Upton, Z. M., J. J. Pulli, B. Myhre, and D. Blau (2006). A reflected energy prediction model for long-range hydroacoustic reflection in the oceans, *J. Acoust. Soc. Am.* **119,** 153–160.

Weary, S. E., W. J. Ozeroff, J. L. Sperling, B. Collins, C. W. Lowery, and S. K. Obermiller (1981). Operation WIGWAM, *Technical Rept. DNA 600F*, 1 September 1981, Defense Nuclear Agency, 266 pp.

Worcester, P. F., and R. C. Spindel (2005). North Pacific acoustic laboratory, *J. Acoust. Soc. Am.* **117,** 1499–1510.

Worcester, P. F., B. D. Cornuelle, M. A. Dzieciuch, W. H. Munk, B. M. Howe, J. A. Mercer, R. C. Spindel, J. A. Colosi, K. Metzger, T. G. Birdsall, and A. B. Baggeroer (1999). A test of basin-scale acoustic thermometry using a large-aperture vertical array at 3250-km range in the eastern North Pacific Ocean, *J. Acoust. Soc. Am.* **105,** 3185–3201.

Vincenty, T. (1975). Direct and inverse solutions of geodesics on the ellipsoid with applications of nested equations, *Surv. Rev.* **176,** 88–93.

Applied Physics Laboratory
University of Washington
1013 N.E. 40th Street
Seattle, Washington 98105-6698
dushaw@apl.washington.edu

Manuscript received 20 January 2015;
Published Online 30 June 2015